J Mater Sci (2006) 41:6599–6609
DOI 10.1007/s10853-006-0199-0

Intra-laminar cracking in CFRP laminates: observations and modelling

N. Balhi · N. Vrellos · B. W. Drinkwater · F. J. Guild · S. L. Ogin · P. A. Smith

Published online: 8 August 2006

Abstract Matrix cracks in composite laminates are almost invariably the first damage mechanisms in composite laminates and are the precursor to more serious forms of damage. The results presented in this paper include experimental investigations into the occurrence of these cracks in a wide range of laminates containing various angle-plies. Ultrasonic detection of these cracks using polar backscattering is found to be successful and shows promise as a method which could be applied outside the laboratory. Further work includes finite element simulations which lead to an understanding of aspects of the accumulation of damage in composite laminates.

Introduction

Intra-laminar matrix cracking is the most common damage to form when a composite laminate is loaded. These intra-laminar cracks are small and difficult to detect using conventional inspection techniques. Moreover there is no agreement as to the conditions under which cracks will form, especially under combined (transverse tension and shear) loading. Although their presence at low crack densities may be acceptable, a high density of intra-laminar cracks is associated with the development of critical failure events such as delamination. The detection of these cracks and measurement of crack density is vital to ensure the structural integrity of composite laminates.

It is now well established that traditional failure criteria, such as those due to Tsai-Hill and Tsai-Wu, are unable to deal satisfactorily with the complexities of matrix cracking, such as the dependence of the strain to first cracking on ply thickness. Much work has focussed on failure criteria based on fracture mechanics which has been shown to predict cracking successfully in the 90° ply of laminates of the type $[0_m/90_n]_s$ and $[\pm\ \theta_m/90_n]_s$ where there is no shear component to the 90° ply stress state [1–5]. A more complex situation is presented by cracking in off-axis plies for other angles, where cracking occurs as a consequence of mixed mode loading. In work on unbalanced $[0/\theta/0]$ GFRP coupons [6], it was shown that the in situ ply stresses at crack formation depend on whether there is a pre-existing defect present in the off-axis ply. When no defect was present, the ply stress state at crack formation was incompatible with currently proposed interactive failure criteria, both stress-based (e.g. Tsai-Hill) and fracture mechanics-based [7]. With a defect present, crack formation was governed by the mode 1 transverse tensile stress component for off-axis ply angles in the range 90° to 45°. The results in this paper extend the work to CFRP. Experimental investigations have been carried out to describe the development of the cracking, with associated closed form analyses. The possibility of detecting of the cracks using ultrasonics has been investigated and finite element-based models of cracked laminates have been developed.

N. Balhi · B. W. Drinkwater
Department of Mechanical Engineering, University of Bristol, Queen's Building, Bristol BS8 1TR, UK

F. J. Guild (✉)
Department of Materials, Queen Mary, University of London, London E1 4NS, UK
e-mail: f.guild@qmul.ac.uk

N. Vrellos · S. L. Ogin · P. A. Smith
School of Engineering, University of Surrey, Guildford, Surrey GU2 7XH, UK

Experimental methods and analysis of results

Materials

The material used in this work is IM7/8552 carbon fibre/epoxy resin. The laminates were made from unidirectional prepreg, 0.125 mm nominal thickness, autoclave moulded by QinetiQ, Farnborough. A range of laminates were manufactured, providing both different off-axis ply angles and different off-axis ply thicknesses. The laminates used to obtain the mechanical testing results presented here were unbalanced lay-ups of the type $[0_2/\theta_8/0_2]$ where $\theta = 45°$, 60°, 75° and two types of cross-ply laminates with different ply thickness, namely $[0_2/90_8/0_2]$ and $[0/90]_{4s}$. Results from ultrasonic detection also included inspection of quasi-isotropic laminates with different ply thickness namely $[0/90 \pm 45]_s$ and $[0_2/90_2/\pm 45_2]_s$. Further laminates used for analysis of the experimental results were a $[\pm 45]_{4s}$ laminate for determination of non-linear shear behaviour and an unbalanced [0/90] beam for determination of thermal strains.

Mechanical testing

For the $(0/90)_{4s}$, $(0_2/\theta_4)_s$ and quasi-isotropic material, rectangular test coupons 250 mm long by 20 mm wide were cut from the original panels using a diamond wheel saw with water lubrication. The edges of all coupons were polished to a 1 μm finish using a Struers Pedemax-2 grinding polishing machine. Polishing the edges provides a consistent sample condition, while facilitating crack observation during testing. Aluminium alloy end-tabs were bonded to all the coupons to minimize damage in the grips of the tensile testing machine during loading. For the unbalanced $(0_2/\theta_4)_s$ coupons, oblique end-tabs were used to minimise gripping constraints due to extension-shear coupling. Oblique end tabs have been used by others [8, 9] when testing off-axis unidirectional composites. Modifying the Sun and Chung approach [8] to the case of a laminate, the angle ϕ for the oblique end-tabs is given by

$$\varphi = \tan^{-1} - \frac{1}{\left(\frac{A_{16}^{-1}}{A_{11}^{-1}}\right)} \quad (1)$$

where A_{16}^{-1} and A_{11}^{-1} are components of the inverse laminate extensional stiffness matrix. The calculations showed the importance of using the laminate values of inverse laminate extensional stiffness; use of the values for the off-axis ply alone introduced significant error (typically a difference of 5° in the calculated optimal angle).

Quasi-static tests were carried out to investigate the initiation and propagation of individual matrix cracks and subsequent crack multiplication. For crack initiation experiments, coupons were tested with polished edges, whereas crack propagation experiments, which have been carried out only on the $[0_2/\theta_4]_s$ coupons, required the off-axis central plies to be notched. A 0.8 mm drill bit was used to drill holes, 3 mm deep, parallel to the direction of the fibres in the (off-axis) centre plies, without damaging the outer 0° plies. A total of 12 notches, six on each edge, were drilled for $[0_2/\theta_4]_s$ coupons (see Fig. 1a, b). In addition, for the $[0_2/45_4]_s$ laminate, further coupons were made where the notches in the central off-axis ply measured 10 mm in depth (Fig. 1c), with a total of six notches, three on each edge. In all cases, the notches were drilled on alternating sides of the coupons in such a way that each crack would develop a distance of at least 10 mm apart from the neighbouring crack on the same edge. This distance was chosen so that the cracks would not interact with each other. Quasi-static tensile tests were carried out to progressively higher strains by loading the coupons to a specific strain level, unloading, and then re-loading to a higher strain. Tests were carried out in displacement control using a displacement rate of 0.5 mm per minute. Strains were measured using longitudinal and transverse strain gauges bonded on both sides of the specimens with cyanoacrylate glue. Edge microscopy and X-radiography were used to monitor the crack development during the strain increments.

Tension–tension fatigue tests were carried out using an Instron 1341 servo hydraulic fatigue machine employing a sinusoidal waveform at a frequency of 10 Hz with an R-ratio of 0.1. Experiments were carried out using the notched $[0_2/\theta_4]_s$ laminates. A peak stress level of approximately 65% of the initial cracking stress has been used for each of the lay-ups tested. Crack length as a function of cycle number has been monitored using X-radiography.

Closed form analysis of stress state at crack onset

The experiments gave results for the stresses (strains) at which cracks first propagated from the notches in the notched coupons, and the stresses (strains) at which crack initiation and (instantaneous) propagation occurred in the unnotched coupons with polished edges. Laminated Plate Theory (LPT) was used to determine the corresponding stress states in the plies undergoing cracking. For the 90° plies in cross-ply and multi-ply laminates there is no shear stress component associated with the principal material directions and so the cracking essentially occurs under mode 1 loading, driven by the transverse normal stress σ_2, while for other off-axis angles the shear stress is non-zero and cracking occurs under mixed mode loading, under the action of the transverse normal stress σ_2, and the in-plane shear stress τ_{12}.

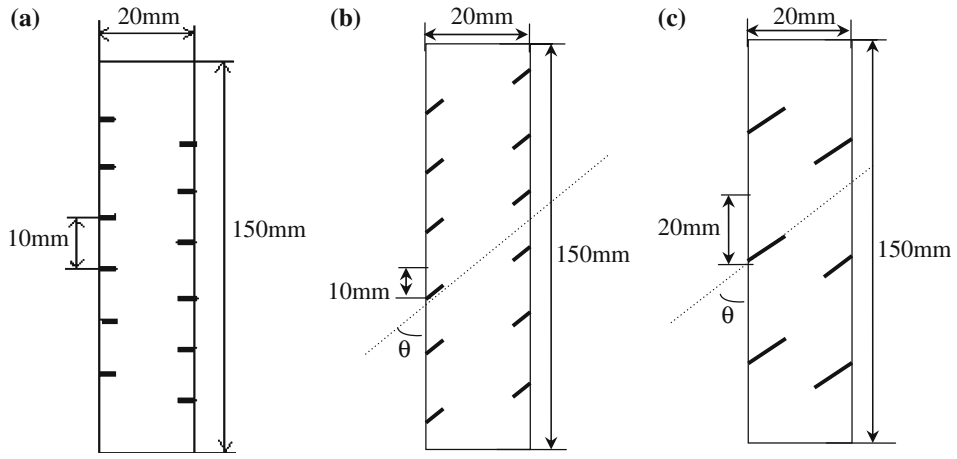

Fig. 1 Schematic of (**a**) $(0_2/90_4)_s$ specimen [3 mm notch depth], (**b**) $(0_2/45_4)_s$ specimen [3 mm notch depth] and (**c**) $(0_2/45_4)_s$ specimen [10 mm notch depth]

Various LPT calculations were carried out using the commercial LAP software. The results for the ply stress states at crack onset reported here were obtained incorporating the non-linear behaviour of the material in shear, which was deduced from the tensile tests on the $[\pm 45]_{4s}$ coupons, and the effect of the residual thermal stress, which was determined from the analysis of measurements on unbalanced beam specimens.

Ultrasonic detection

Transverse cracks within composite laminates are extremely difficult to detect using normal incidence ultrasound since the plane of the crack is parallel to the ultrasonic beam. A number of authors (see for example [10]) have shown that improved sensitivity can be obtained by orienting the ultrasonic beam with respect to the surface normal. Using this approach, termed polar backscatter, inhomogeneities, such as the matrix–fibre interface, fibre bundles and cracking cause ultrasound to be scattered back to the transducer. Vertical cracks behave like strong scatterers, causing high amplitudes to be reflected back to the transducer. In a series of experiments, a range of incident angles (measured with respect to the surface normal) between 15° and 50° were investigated. An incidence angle of 20° was found to provide the best contrast between cracked and uncracked regions. This corresponds to a longitudinal wave propagating at close to 45° in the composite, although the precise angle will vary from layer to layer within the section. The contrast of the scan image was further improved if the data collection gate was positioned to receive the ultrasound forward scattered from the crack and reflected from the back surface to the transducer. The experimental configuration is shown schematically in Fig. 2. The ultrasonic 'ray' indicates the path of the ultrasound and the primary direction of scattering from the crack. From this it can be seen that the crack behaves more like a reflector and hence scattering strongly towards

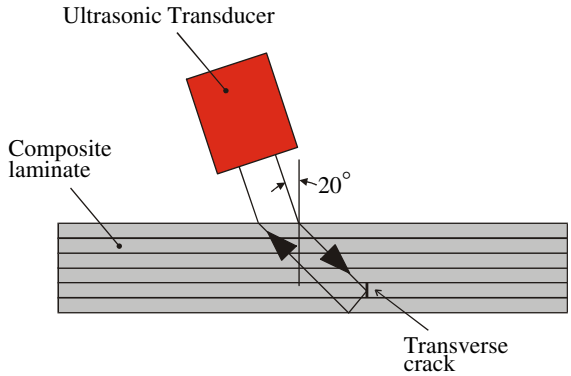

Fig. 2 Schematic view of the ultrasonic polar backscatter technique showing the path of an ultrasonic 'ray'

the back face, then back to the transducer. The low attenuation of the composite and the thin sections inspected meant that a relatively high ultrasonic frequency (25 MHz) was used. This equates to a wavelength of 0.13 mm in the composite laminate.

Finite element simulations

Matrix crack growth in CFRP laminates has been simulated using finite element analysis. The package used was ABAQUS Standard (Implicit code) version 6.4. For cross-ply laminates, the models could be drawn in two dimensions in the thickness-axial plane using generalised plane strain elements. For these two-dimensional models, only crack growth across the whole width could be simulated. Angle-ply laminates require full three-dimensional finite element models to simulate both mechanical properties and crack growth across the width. The simulations for increasing crack density were carried out using symmetry condition on meshes with reduced length. Linear material properties were used, but geometric non-linearity was included in all the models.

The energy release rate for isolated transverse cracks in the angle-ply unbalanced laminates has been investigated using three-dimensional finite element simulations. The cracks are assumed to span the entire thickness of the cracked ply. The geometry of the models takes into account the oblique end tabs used in the mechanical testing to accommodate extension-shear coupling; results from finite element simulations confirmed the accuracy of the calculations described in the earlier ''Mechanical testing'' section. Non-linear geometry was implemented for all the laminates, to take into account any specimen rotation in its plane. The applied strain used for the simulations was the applied mechanical strain for crack propagation found in the experiments. The total strain energy release rate arising from crack growth can be calculated from results from the whole model. This can be carried out using the energy approach; the total strain energy can be extracted as a variable from the simulations. Alternatively, the well-known compliance change approach can be used. It was confirmed that both methods gave the same results.

Simulation of incremental crack growth requires very fine meshes for accuracy. These meshes can only be attained using sub-modelling, which is carried out in two stages. The first global model represents the whole structure to be analysed, including the important geometric and property details of the structure, but with a coarse mesh which would not be able to reflect local stress variability. The displacements from the global model are used to load the detailed model including the area of interest, which can now be drawn using a suitable fine mesh.

Finite element analysis has been used to investigate the proportions of modes I and II for crack propagation in off-axis laminates. The method used is virtual crack closure [11, 12], based on the concepts of linear elastic fracture mechanics. This is implemented using two simulations, before and after the increment of crack growth. The forces associated with the nodes to be released in the increment of crack growth are found in the first analysis. In the second analysis, after release of these nodes, the displacements of the nodes are found. Thus the virtual energy required to close the crack can be calculated, and this is considered equal to the energy required to open the crack. Thermal stresses are not included in these simulations. The values of strain energy release rate were found to be dependent on the elements and meshes used; all results presented here have been obtained following mesh convergence studies.

Results

Crack formation

The stresses (strains) at which cracks first propagated from the notches in the notched coupons, and the stresses (strains) at which crack initiation and (instantaneous) propagation occurred in the unnotched coupons with polished edges were measured carefully. For the unnotched coupons from the $[0_2/\theta_4]_s$ lay-ups with polished edges the crack formation was instantaneous with cracks propagating across the thickness and width of the off-axis ply in an unstable manner. The associated crack morphology was complex, suggesting considerable energy release during crack formation. In the $[0_2/90_4]_s$ specimens, first cracking was seen at an applied longitudinal strain of about 0.8%. For lay-ups with the central plies oriented at other off-axis angles, it was found that the strain for first cracking increased with decreasing off-axis angle. For the $[0_2/45_4]_s$ lay-up there was no matrix cracking in the central layer prior to laminate failure by fracture of the fibres in the 0° layers at an applied longitudinal strain of 1.1% or greater. Figure 3 shows the initial cracking strain in the unnotched $[0_2/\theta_4]_s$ lay-ups as a function of off-axis angle (upper trend line).

In the notched $[0_2/\theta_4]_s$ lay-ups, where the pre-existing defect spanned the thickness of the off-axis central layer, crack growth occurred rapidly in the specimens with high off-axis angles, i.e. as the strain was increased in steps of 0.1%, cracks grew from the starter notches across the entire coupon width. There were also some cracks formed away from the notches. This is apparent in Fig. 4, which shows a series of X-radiographs for a $[0_2/75_4]_s$ specimen. For specimens from lay-ups with lower off-axis angles, there was evidence of more progressive crack growth, i.e. cracks which propagated from notches did not always extend across the full width of the coupon immediately, but grew with increasing strain. This aspect of the crack propagation behaviour can be seen in Fig. 5, which shows a series of X-radiographs for a $[0_2/45_4]_s$ specimen. There was no apparent difference in the behaviour of the $[0_2/45_4]_s$ specimens with the two different initial notch lengths (3 mm and 10 mm). Crack propagation occurred at similar strains in each case.

The data for the strains at which crack propagation first occurred in the various lay-ups are shown in Fig. 3. Overall

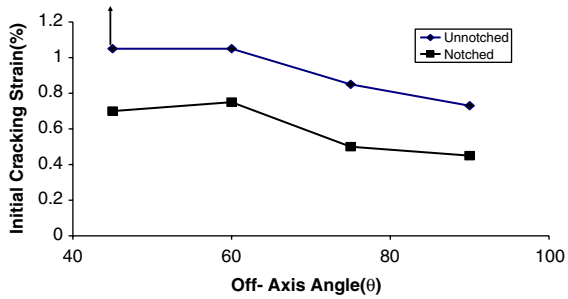

Fig. 3 Applied longitudinal strain for off-axis ply crack formation as a function of ply angle for unnotched (polished edges) and notched coupons from $[0_2/\theta_4]_s$ laminates

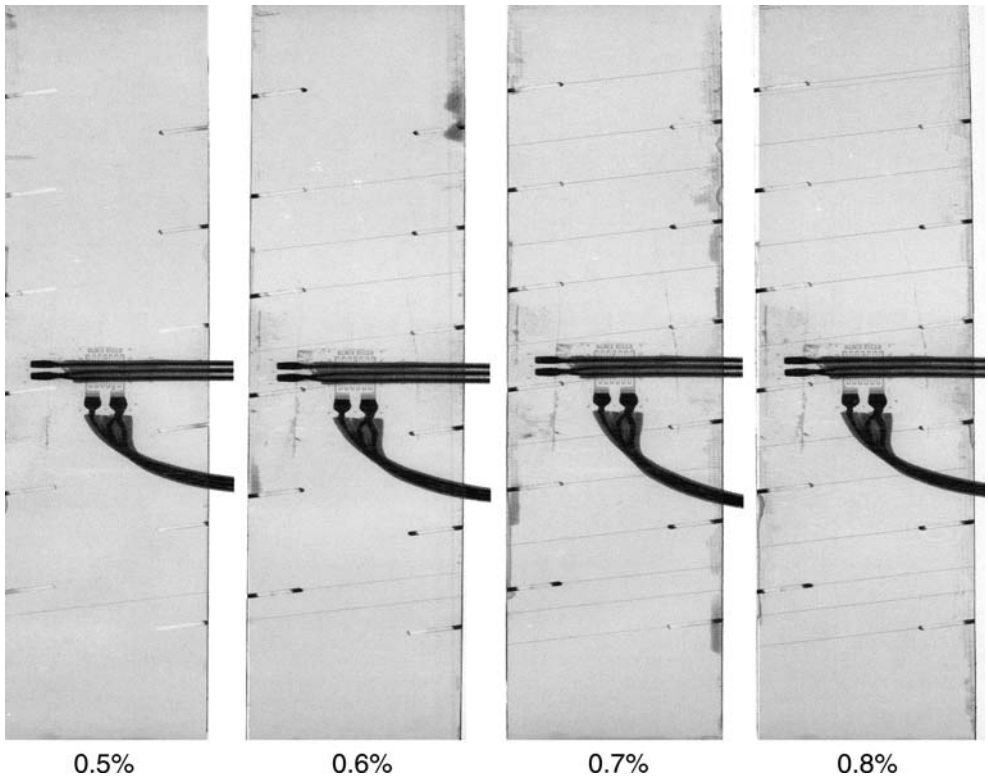

Fig. 4 Dye-penetrant enhanced X-radiographs of a notched $[0_2/75_4]_s$ coupon showing crack development with increasing applied longitudinal strain

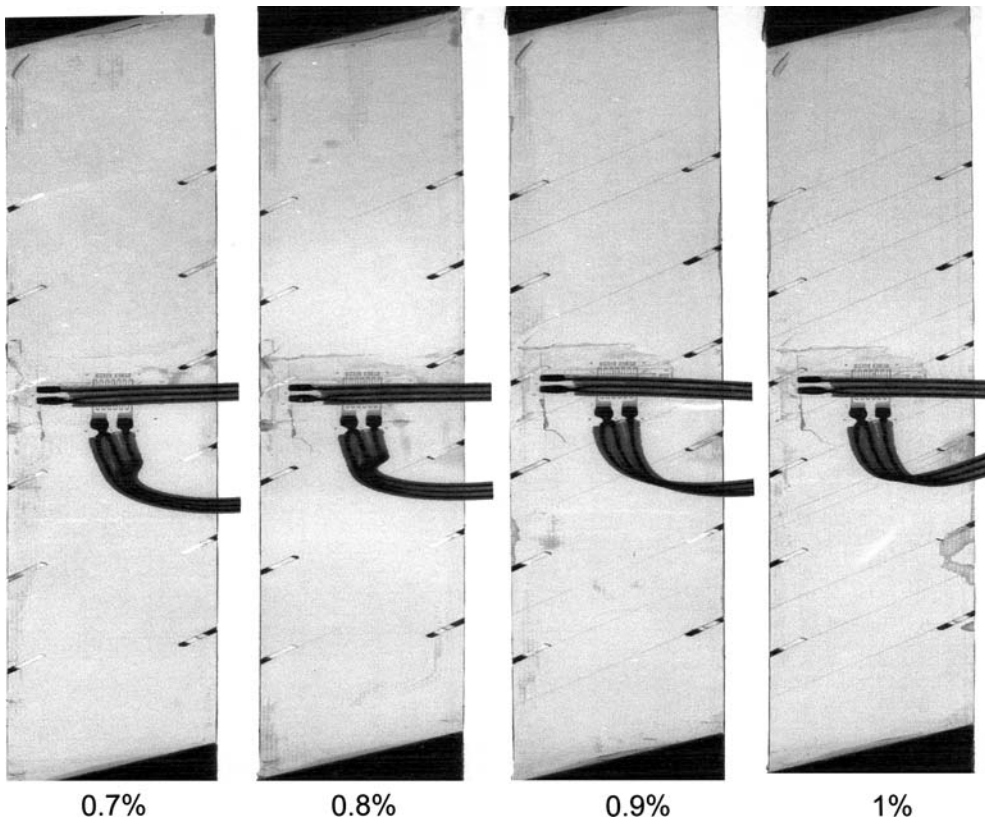

Fig. 5 Dye-penetrant enhanced X-radiographs of a notched $[0_2/45_4]_s$ coupon showing incremental crack growth with increasing applied longitudinal strain

(and in accordance with the results of Crocker et al. 1997 [6] for GFRP coupons containing off-axis plies) the data show that crack propagation in coupons with notches occurred at lower strains than crack initiation in the unnotched coupons.

Results from the LPT analysis of the $[0_2/\theta_4]_s$ laminates are shown in Fig. 6 as a plot of transverse normal stress against the corresponding ply shear stress at off-axis ply crack formation in notched and unnotched $[0_2/\theta_4]_s$ CFRP coupons. The results show that for both the unnotched and notched specimens the transverse normal stress σ_2 value corresponding to initial cracking is similar for the $[0_2/90_4]_s$, $[0_2/75_4]_s$ and $[0_2/60_4]_s$ samples, with the notched values some 20 MPa lower than the unnotched values. Interestingly, the behaviour of the $[0_2/45_4]_s$ laminates is somewhat different, in that for crack propagation from notches in these laminates there appears to be a significantly reduced value of σ_2, implying that there is an interaction between the transverse normal and shear stress components which promotes crack propagation. It is not possible to comment upon whether there may be a similar effect in the unnotched $[0_2/45_4]_s$ coupons, since laminate failure occurred before any off-axis ply cracking was seen in these laminates. In previous work on GFRP laminates, the transverse normal stress value for crack propagation was similar for a range of $[0/\theta/0]$ type laminates, with $\theta = 45^o$, 54^o, 75^o and 90^o [6].

Crack accumulation and residual properties

Accumulation of matrix cracks is well known to lead to a reduction in the mechanical properties of composite laminates.

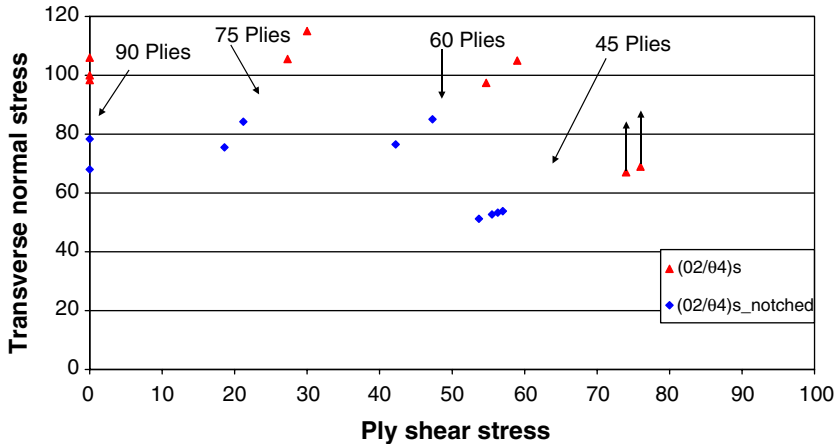

Fig. 6 Plot of transverse normal stress as a function of the corresponding ply shear stress at off-axis ply crack formation in notched and unnotched $[0_2/\theta_4]_s$ CFRP specimen. (Values based on non-linear laminate analysis including thermal stresses)

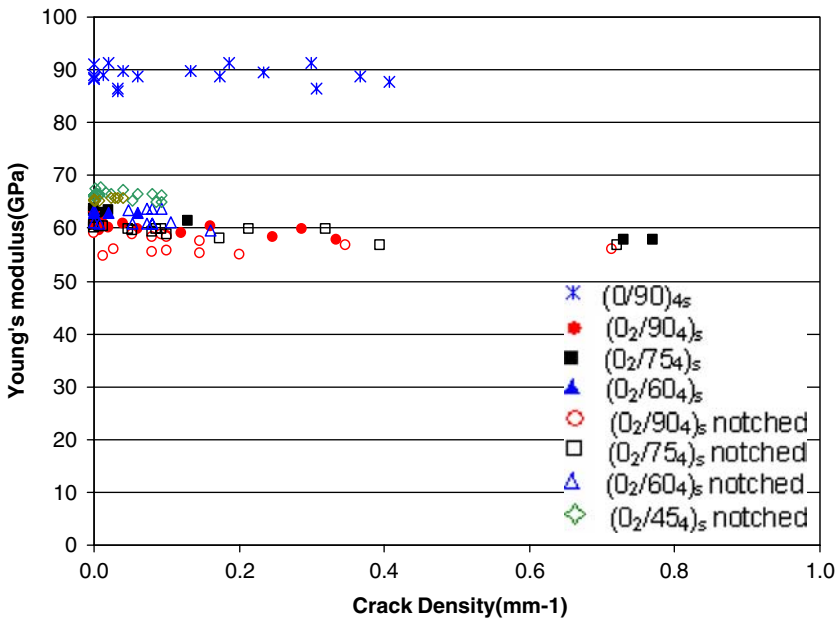

Fig. 7 Young's modulus as a function of off-axis ply crack density for the range of $[0_2/\theta_4]_s$ specimens tested

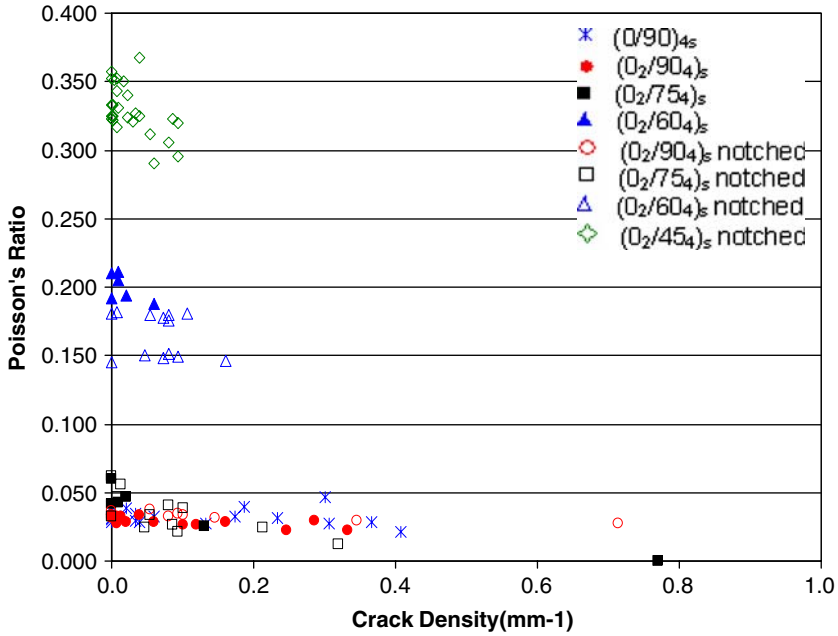

Fig. 8 Poisson's ratio as a function of off-axis ply crack density, for the range of $[0_2/\theta_4]_s$ specimens tested

The results shown here, Figs. 7 and 8, give the change in Young's modulus and Poisson's ratio with increasing crack density for the cross-ply laminate, $[0_2/90_4]_s$, and the angle-ply laminates, $[0_2/\theta_4]_s$ where $\theta = 45°, 60°$ and $75°$. There is a degree of variability in both plots, but it should be noted that there is no difference between the results for the notched specimens and those with polished edges. The Poisson's ratio is difficult to measure experimentally as the transverse strains are small and sensitive to the degree of alignment of the transverse gauge. A trend of property reduction with increasing crack density is apparent, especially for the Poisson's ratio.

Crack growth in fatigue

Crack growth observations were made for each of the four laminate configurations $(0_2/\theta_4)_s$ (where $\theta = 45°$, $60°$, $75°$ and $90°$). In each case, notches were machined into the samples. In contrast to the quasi-static tests, all the cracks for each laminate configuration propagated from notches in fatigue, and no cracks were observed to develop away from the notches. Crack growth as function of the number of cycles was recorded for each configuration, and an example is shown in Fig. 9 for crack growth in a $(0_2/75_4)_s$ coupon specimen. In this example, cracks began to grow from the

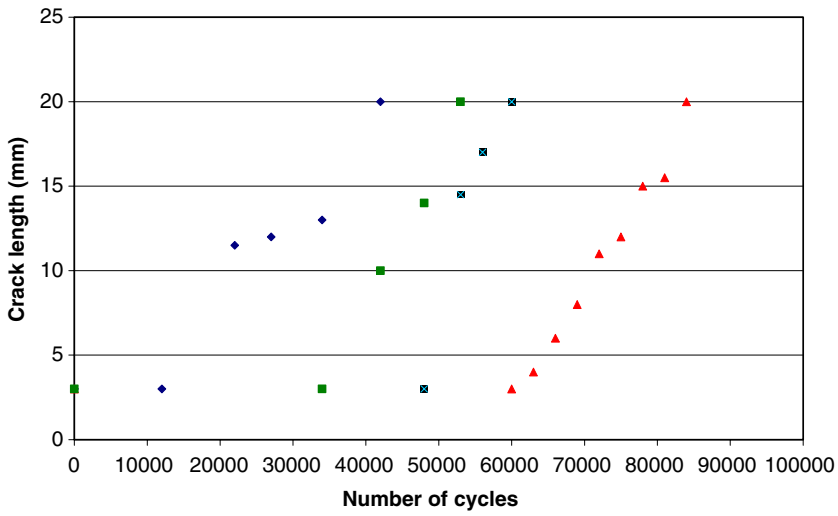

Fig. 9 Plot of crack length against number of cycles for a (0/75/0) CFRP coupon under fatigue loading (data relating to the growth of four cracks are shown)

notches after widely varying numbers of cycles, in the range from 12,000 to 60,000 cycles. The crack growth rate for each crack was roughly constant, however, at about 10^{-3} mm cycle^{-1}. This behaviour was consistent across all the samples tested—once the cracks had started to propagate, the increase in crack length appears to be roughly linear with number of cycles. No delaminations were associated with any of the matrix cracks in any of the tests.

The results described here for matrix crack growth in the off-axis plies of CFRP are similar to the results of Crocker [13] who also tested unbalanced (0/θ/0) coupon configurations, but in GFRP (E-glass fibres and Shell 'Epikote' 828 epoxy resin). Qualitatively, the major difference between the CFRP and GFRP coupons is that the crack growth was seen to be more uniform in GFRP, in particular there was less variability in the ''incubation'' times for cracks to start to propagate from the notches.

Ultrasonic crack detection

The ultrasonic polar backscatter technique described in Section ''Ultrasonic detection'' enables closely spaced individual cracks to be imaged from which the crack density can be assessed. Figure 10 shows the resulting polar backscatter scans for a $[0_2/90_4]_s$ and a $[0_2/75_4]_s$ coupon. A dense cracking pattern is observable, from which it is relatively simple to perform a transverse matrix crack count. Cracks detected using this ultrasonic technique agreed well with those obtained using dye penetrant X-rays such as those shown in Figs. 4 and 5.

The most significant polar backscatter experimental result was the detection of transverse cracking in the outer 90° layers of a $[0/90/+45/-45]_S$ laminate. The cracking can be seen when inspected from either side. Individual cracks were resolved in this 0.125 mm layer (overall laminate thickness 1 mm); an example is shown in Fig. 11. The detection of such small cracks demonstrates the potential of this inspection technique for accurate assessment of the structural integrity of composite laminates.

The effect of the X-ray dye penetrant used to detect cracks (see for example, Figs. 4, 5) on the ultrasonic detectability of intra-laminar cracks was investigated. Figure 12 shows an example of the results obtained from cross-ply coupons, $[0_2/90_4]_s$, with 1 mm deep intra-laminar cracks. The results in Fig. 12 show that the addition of the dye penetrant caused an immediate and noticeable reduction in the performance of the ultrasonic polar backscattered technique. The performance was measured by comparing the maximum signal amplitude in a region where there was an observable crack (A_{crack}) with an averaged value from an uncracked region ($A_{\text{uncracked}}$). The signal-to-noise-ratio was defined as

$$\text{SNR} = \frac{A_{\text{crack}}}{A_{\text{uncracked}}} \tag{2}$$

This signal-to-noise-ratio can also be used as a measure of the detectability of a given crack. Dye penetrant was added to three separate specimens and in all cases a decrease in detectability to around 40% was found after about 24 h following application of the dye penetrant. The results in

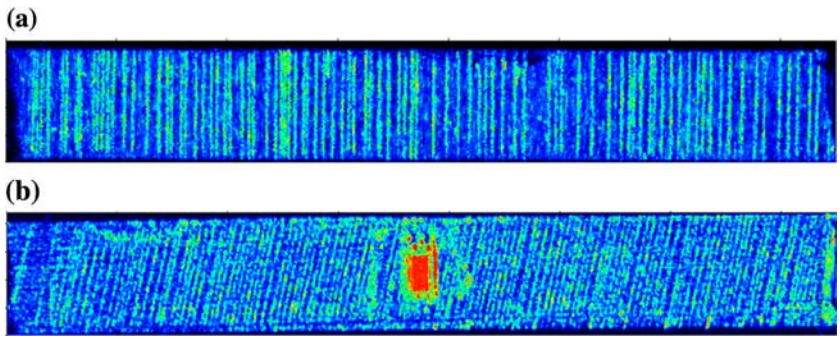

Fig. 10 Polar backscattering C-scan of (150 × 20) mm coupons with transverse cracking. Note that the strong signal in the centre scan (**b**) is from a strain gauge and should be ignored: (**a**) $[0_2/90_4]_s$ and (**b**) $[0_2/75_4]_s$

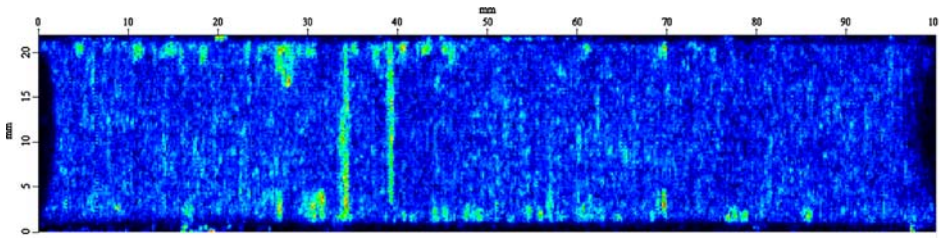

Fig. 11 Polar backscattering image at 20° incidence angle on $(0/90/+45/-45)_S$ laminate with cracking in the top 90° layer

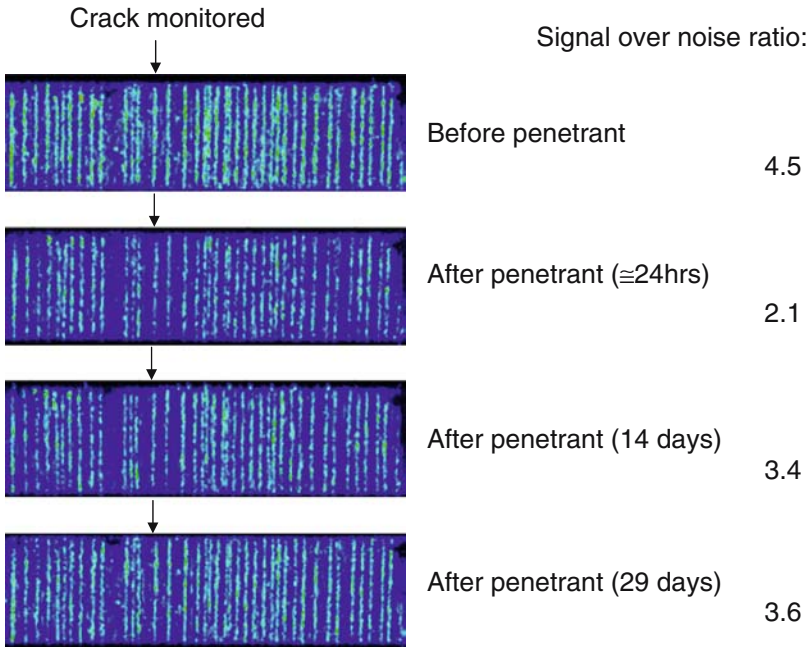

Fig. 12 Effect of dye-penetrant on crack detection in $[0_2/90_4]_s$

Fig. 12 show the decrease of this effect with time; the ultrasonic detectability has recovered to 75% of the detectability prior to the penetrant after 14 days and 80% after 29 days. It does not seem credible that the penetrant could have evaporated from within these internal cracks; it must have been absorbed. These results may be highly significant for the use of dye penetrant and subsequent crack growth experiments.

Comparisons with finite element simulations

Crack growth across the width

The process of crack growth across the width for single cracks has been examined. The variation of total strain energy for crack growth in the $[0_2/45_4]_s$ laminates is shown in Fig. 13. These simulations were carried out for the notched crack propagation strain observed experimentally (Fig. 3) and the total strain energy release rate was calculated using the global method. The results suggest that there is some dependence of energy release rate upon crack length with the value of strain energy release rate being reduced at smaller crack lengths. This is somewhat in contrast to the results for other lay-ups, in particular the cross-ply, for which the value of energy release rate is more independent of crack length. It is difficult to relate these calculations to the results from the quasi-static tests. Because the quasi-static tests were carried in displacement control (as opposed to load control), the load tends to decrease as cracks propagate and in this situation the numerical simulation ceases to represent the experiment. These numerical results are certainly consistent, however, with the results from the fatigue tests in that crack growth rates from pre-cracks of several millimetres in extent were independent of crack length.

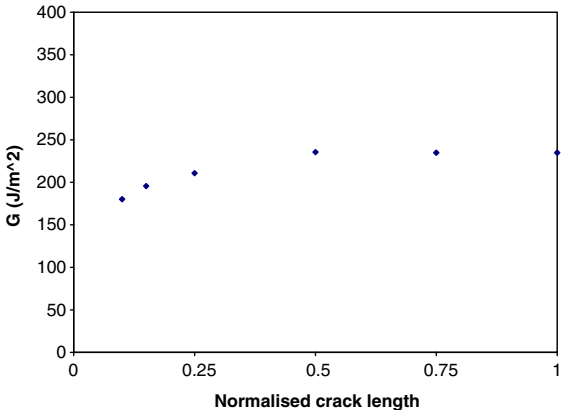

Fig. 13 Variation of total strain energy release rate for crack growth across the width of $[0_2/45_4]_s$ laminate

Strain energy release rate for single cracks

The process of single crack growth in the $[0_2/45_4]_s$ laminates has been examined in detail. These simulations were carried out for the notched crack propagation strain observed experimentally (Fig. 3). The strain energy release rate has been calculated both from the global approach and, using sub-models, the virtual crack growth method. Results

for crack growth with the crack existing half way across the width are shown in Fig. 14.

Figure 14 shows consistent numbers for the average value of total strain energy release rate calculated globally or locally. This is a reassuring result which confirms the validity of both methods used. The virtual crack growth method has been used to assess the mode mixity of the crack growth. The results in Fig. 14 show that the crack growth is nearly equally half in Modes I and II. The variability across the laminate thickness indicates the dependence of the strain energy values; as expected, the contribution from the ply nearest the 0° ply is smaller than the contribution from the centre ply. This arises from the constraint on the displacement imposed by the 0° ply. The shape of this variability indicates that crack growth would always be expected to extend across the thickness of the ply since the highest value of strain energy release rate is at the centre of the ply. This confirms the experimental observation that cracks always span the entire thickness of plies.

Further simulations for crack growth half-way across the width have been carried out for cross-ply laminates, $[0_2/90_4]_s$, and one other angle-ply laminate, $[0_2/75_4]_s$. The values of applied strain in the simulations have matched the values of crack propagation strain observed experimentally (Fig. 3). Crack growth in the cross-ply laminate was found to be all Mode I, as expected; for the $[0_2/75_4]_s$ laminate a small proportion of crack growth, around 7%, was found in Mode II; as shown in Fig. 14, for the $[0_2/45_4]_s$ laminate around 50% was found in Mode II. Interestingly, the values of Mode I contributions to fracture energy for all three laminates were approximately equal, indicating that the crack growth is dependent only on the Mode I strain energy release rate. However, this result must be considered with caution since the complexity of the analyses did not allow thermal strains to be taken into account.

Residual properties

The residual properties arising from increasing crack density have been predicted using three-dimensional finite element models of decreasing length. The results for normalised stiffness are shown in Fig. 15; the results for the three angle-ply laminates are shown. The finite element results, denoted by the trend lines in Fig. 15, show the expected trend with the angle of the ply. The lower angle plies are stiffer and carry a greater proportion of the load; hence, cracking in these lower angle plies causes more overall stiffness reduction. The predicted variability with crack density is nearly linear. The experimental results are rather scattered with no apparent differences in normalised values between the angle plies; the overall trends in experimental results are in agreement with the predictions. The experimental scatter is not surprising since the actual stiffness change measured is very low for all these laminates.

The results for normalised values of Poisson's ratio for the three angle-ply laminates are shown in Fig. 16. The finite element results, denoted by the trend lines in Fig. 16, show the same trend with the angle of the ply as found for the stiffness results (Fig. 15) as expected. However, the predicted variability is not linear; changes in high values of crack density have a greater effect on the value of Poisson's ratio than changes in low values of crack density. This implies more interaction between neighbouring cracks in respect of transverse (as opposed to longitudinal) strains. The variability of normalised values of Poisson's ratio is about three times greater than the variability of normalised values of stiffness. The overall trends in experimental results are in general agreement with the predictions although there are no apparent differences in normalised values of Poisson's ratio between the different angle plies. It should be noted that a clear difference in actual experimental values was found (Fig. 8).

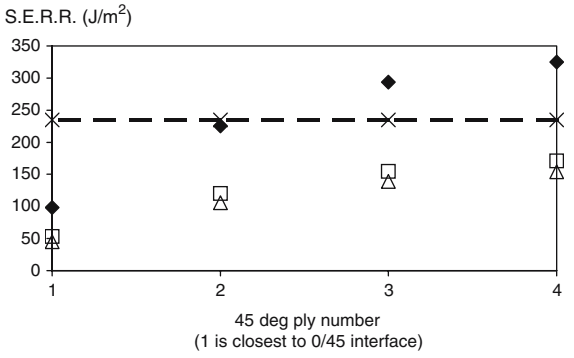

Fig. 14 Strain energy release rate for crack growth in $[0_2/45_4]_s$ laminate, showing variability across the thickness of the laminate

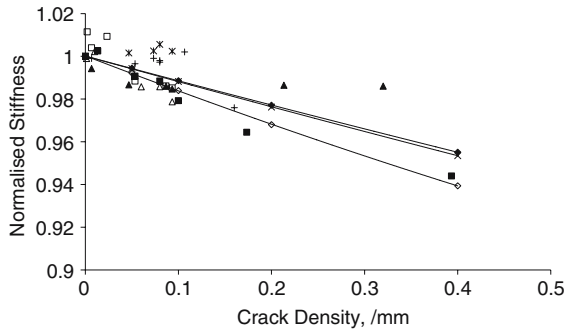

Fig. 15 Predicted change in normalised stiffness with crack density, showing trend lines; comparisons with experimental results. Open symbols: $[0_2/45_4]_s$; crosses: $[0_2/60_4]_s$; closed symbols: $[0_2/75_4]_s$

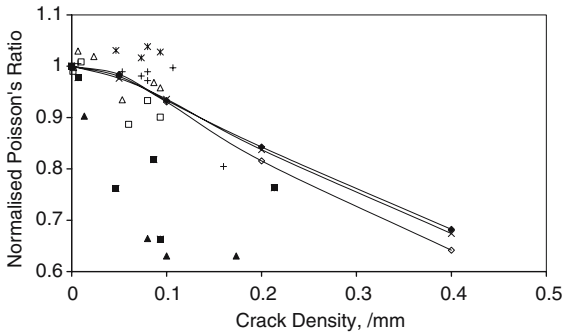

Fig. 16 Predicted change in normalised Poisson's ratio with crack density, showing trend lines; comparisons with experimental results. Open symbols: $[0_2/45_4]_s$; crosses: $[0_2/60_4]_s$; closed symbols: $[0_2/75_4]_s$

Concluding remarks

Matrix cracking in composite laminates is critically related to their structural integrity. Crack initiation and propagation in the off-axis plies of a range of CFRP laminates have been studied. Careful introduction of notches into the central off-axis plies of $(0_2/\theta_4)_s$ laminates has facilitated separation of the initiation and propagation stages of matrix crack formation. The results for $(0_2/\theta_4)_s$ laminates show that for the off-axis angles investigated (i.e. 45°, 60°, 75° or 90°), the applied strain for crack propagation in notched coupons was lower than for crack initiation in coupons with polished edges. Laminate theory has been used to examine the ply stress states at crack onset. It is shown that the transverse normal stress component appears to be the main controlling parameter, although there appears to be a significant shear interaction for cracking of off-axis plies at 45°. It has been shown that these cracks can be accurately detected using ultrasonic scanning at an oblique incidence angle of 20°; this may be an important technique for in-service intra-laminar crack detection. The effect of matrix cracking on the global mechanical properties of unbalanced and cross-ply laminates has been predicted using finite element analysis and compared with the experimental results. The strain energy release rate associated with the crack growth has been found and the importance of mode mixity has been demonstrated.

Acknowledgements We are grateful to the EPSRC and dstl for funding of this work. It is a pleasure to acknowledge useful discussions with our collaborators from dstl, the National Physical Laboratory and QinetiQ.

References

1. Boniface L, Ogin SL, Smith PA (1991) In: O'Brien TK (ed) Composite materials: fatigue and fracture, vol 3. ASTM STP 1110, American Society for Testing and Materials, Philadelphia, p 9
2. Zhang J, Fan J, Soutis C (1992) Composites 23(5):299
3. Varna J, Berglund LA (1992) J Reinforced Plastics Composites 11:709
4. Nairn JA, Hu S, Bark JS (1993) J Mater Sci 28:5099
5. McCartney LN (1998) Compos Sci Technol 58:1069
6. Crocker LE, Ogin SL, Smith PA, Hill PS (1997) Compos Part A 28A:839
7. Shahid I, Chang F-K (1995) J Compos Mater 29:926
8. Sun CT, Chung I, (1993) J Compos Mater 24(8):619
9. Prickett AC (2001). Intralaminar cracking of fibre reinforced composites: a fracture mechanics and ToF-SIMS study. PhD thesis, University of Surrey
10. Bar-Cohen Y, Crane RL (1982), Mater Eval 40:970
11. Irwin GR (1958) Handbuch der Physik, Vol V. Springer-Verlag
12. Rybicki EF, Kanninen F (1977) Eng Frac Mech 9:931
13. Crocker LE (1998) Mixed-node intralaminar fracture in glass/epoxy laminates. PhD thesis, University of Surrey